Supporting Information

Conforti et al. 10.1073/pnas.1715865115

SI Materials and Methods

ZFP-Mediated muHTT Down-Regulation. Constructs were designed as bicistronic vectors carrying a puromycin resistance gene located downstream of the 3′ region of the ZFP coding sequence separated by a "self-cleaving" T2A peptide. Both sequences were cloned into the inducible lentiviral vector FUW-tetO-MCS (#84008; Addgene), linearized with EcoRI-XbaI or EcoRI-HpaI. T2A-puromycin resistance sequence was synthetized as gBlock (Integrated DNA Technologies), flanked by the restriction site BsrGI and AfeI for in-frame cloning into the FUW-tetO-ZFPs plasmid. For subcloning into constitutive plasmids, the ZFPs-T2A-puroR coding sequences were digested from the FUW-tetO-MCS constructs using EcoRI-AfeI and ligated into the pCAG-Cre (#26647; Addgene) recipient plasmid upon excision of Cre by EcoRI-NotI digestion and 5′ blunting at the NotI site. Final clones were verified by Sanger sequencing. ZFPs and CMV-rtTA lentiviruses were produced using a modified protocol from Dull et al. (53). Briefly, 11 × 106 HEK293T cells were plated the day before in 15-cm tissue culture dishes in DMEM + 10% FCS (Thermo Scientific). The next day, the cells were transfected by Calcium Phosphate (50552; Sigma-Aldrich) using the following amount of plasmid per dish: 24 μg FUW-tetO-ZFP-A-T2A-PURO or FUW-tetO-ZFPΔDBD-T2A-PURO or CMV-rtTA; 18 μg of psPAX2 (#12260; Addgene); 6 μg pCMV-VSVg (#8454; Addgene). Medium was replaced after 8 h and viral supernatant collected after additional 24 and 36 h. The virus was filtered (0.45 μm) and concentrated by ultracentrifugation (50,000 × *g* for 2 h). Pellets were briefly dried and suspended in 30 μL HBSS and left over night at 4 °C with gentle rotation. Lentiviral titres were measured by qPCR using serial dilution of the concentrated supernatants (MoBiTeC).

Real-Time qPCR. Primer pairs used were as follows: hOct4A-fw, 5′-AGGCTCTGAGGTGTGGGGGAT-3′; hOct4A-rev, 5′-AGGCGGCTTGGAGACCTCTCA-3′; hOct4B-fw, 5′-AGTGCTGGAATTATAGGCGTGA-3′; hOct4B-rev, 5′- ATAACCTGACAGGTGTTCTCGA-3′; hOct4B1-fw, 5′-TCTGCAGATTCTGACCGCAT-3′; hOct4B-rev, 5′-AGACTACCCTCACCCATGAA-3′; hPax6-fv, 5′- ATGGCAGCTGTGTGTGACACT-3′; hPax6-rev, 5′- GTGGAATTGGTTGGTAGACAC-3′; hGsx2-rev, 5′-AGTGCAGGTGCGAAGTGAC-3′; hAscl1-fv, 5′-TGTGCAAAAGCAGTGGGCTC-3′; hAscl1-rev, 5′- TATTGGGGTGGGGGGCTACTG-3′; hCtip2-fv, 5′-GATGCCAGAATAGATGCCGG-3′; hCtip2-rev, 5′- CGCCACACTGCTTCCTTTTG-3′; hDarpp32-fv, 5′- CTGAGGACCAAGTGGAAGAC-3′; hDarpp32-rev, 5′- GATGTCCCCTCCACTTCCTC-3′; hScn1B-rev, 5′-CTCCTGTGCAGCAGTCTCCGT-3′; hScn2B-fv, 5′-ATAGGAATGGCTTGGTGCAGT-3′; hScn2B-rev, 5′-AGTGCATCAGCAAGCTTCAAT-3′; hScn3B-fv, 5′-AATAGTGCTTGGTGTGCTTGC-3′; hScn3B-rev, 5′- ACTGCATGGCACACTAAAGGT-3′; hScn4B-fv, 5′- AGGCATCTGGAGACTGAGAAA-3′; hScn4B-rev, 5′-ATGGCAGCTGTGTGTGACACT-3′; hTbr2-fv, 5′-CACCGCCACCAAACTGAGAT-3′; hTbr2-rev, 5′- CGAACACATTGTAGTGGGCAG-3′; hTbr1-fv, 5′- AAGCCCAAGGACCTGTCCGA-3′; hTbr1-rev, 5′- GCTGGAGTCGATGGACTTGAT-3′; ZFP-fv, 5′-GGATCCGGCATGGATGCTAA-3′; ZFP-rev, 5′-CTCCTCCCTGGTGAAGTCCA-3′; hHTT-fv, 5′-CGCTATGGAACTTTTTCTGCTGTG-3′; hHTT-rev, 5′-CTGTAACCTTGGAAGATTAGAATCCATC-3′; hGap43-fv, 5′-AGGAAAGGAGAGAAGGCAGGAAGA-3′; hGap43-rev, 5′-TCAACCTGTTTGGTTCTTCTCAT-3′; hCelsr3-fv, 5′-GCTGGCATTTCGGACACG-3′; hCelsr3-rev, 5′-AGAAGGAGATGGGAAGCACGG-3′; hSox11 Hs00846583_s1 (Applied Biosystem); mCelsr3-fv, 5′-GCAGTCCTCAAGCACTCCCTC-3′; mCelsr3-rev, 5′-CCTGGTGGCTCCTCATTCG-3′, mGap43-fv, 5′-GAGGGAGATGGCTCTGCTAC-3′; mGap43-rev, 5′-CACATCGGCTTGTTTAGGC-3′; mSox11 Mm01281943_s1 (Applied Biosystem); hEAR-fv, 5′-GAGGCTGAGGCAGGAGAATCG-3′; hEAR-rev, 5′- GTCGCCCAGGCTGGAGTG-3′; hScn1B-fv, 5′- AAGAAGATCCACATTGAGGTA-3′; 5′-h18S-fv, 5′-CGGCTACCACATCCAAGGAA-3′; h18S-rev, 5′-GCTGGAATTACCGCGGCT-3′; mActin-fv, 5′-AGTGTGACGTTGACATCCGTA-3′; m-Actin-rev, 5′-GCCAGAGCAGTAATCTCCTTCT-3′.

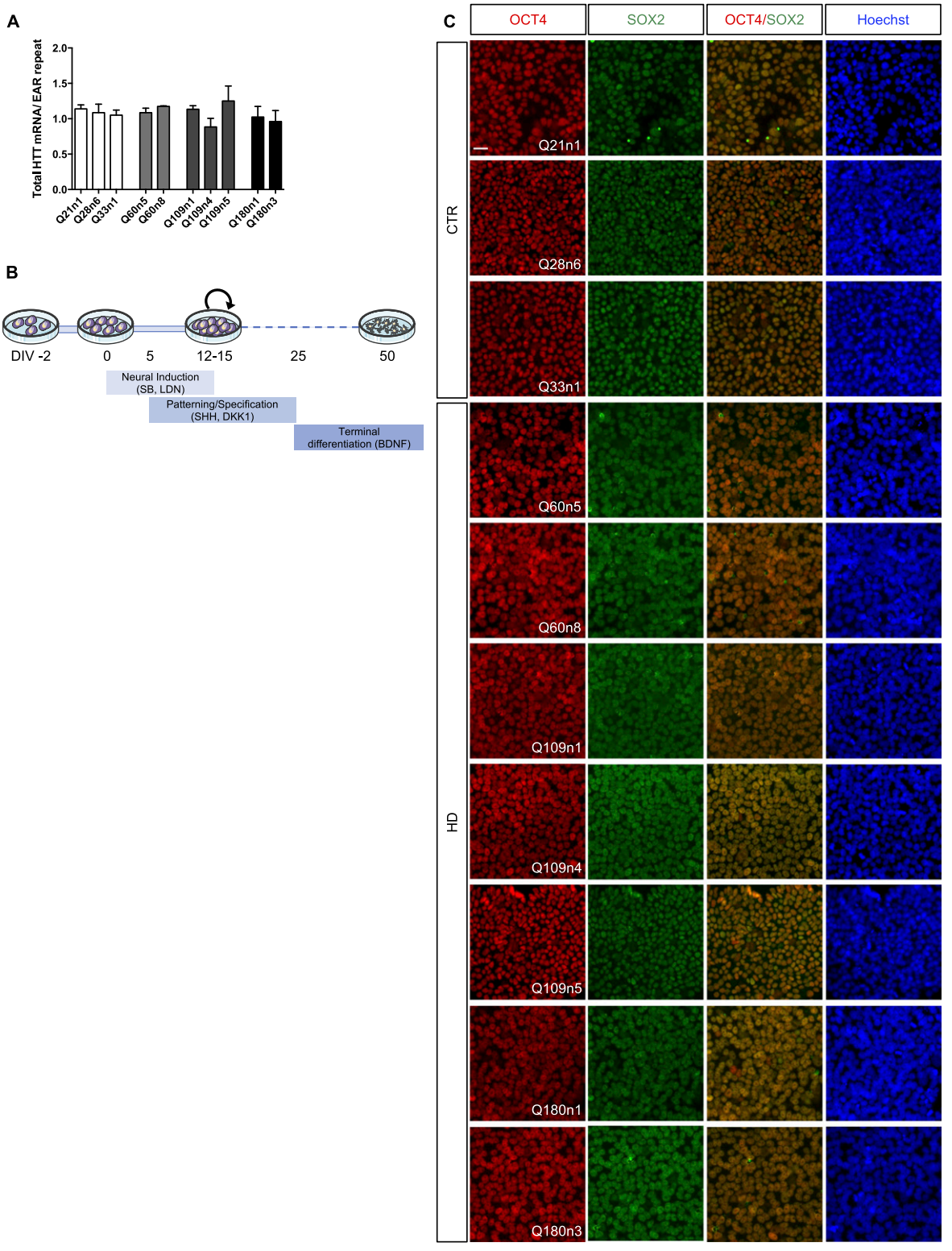

Fig. S1. (Continued)

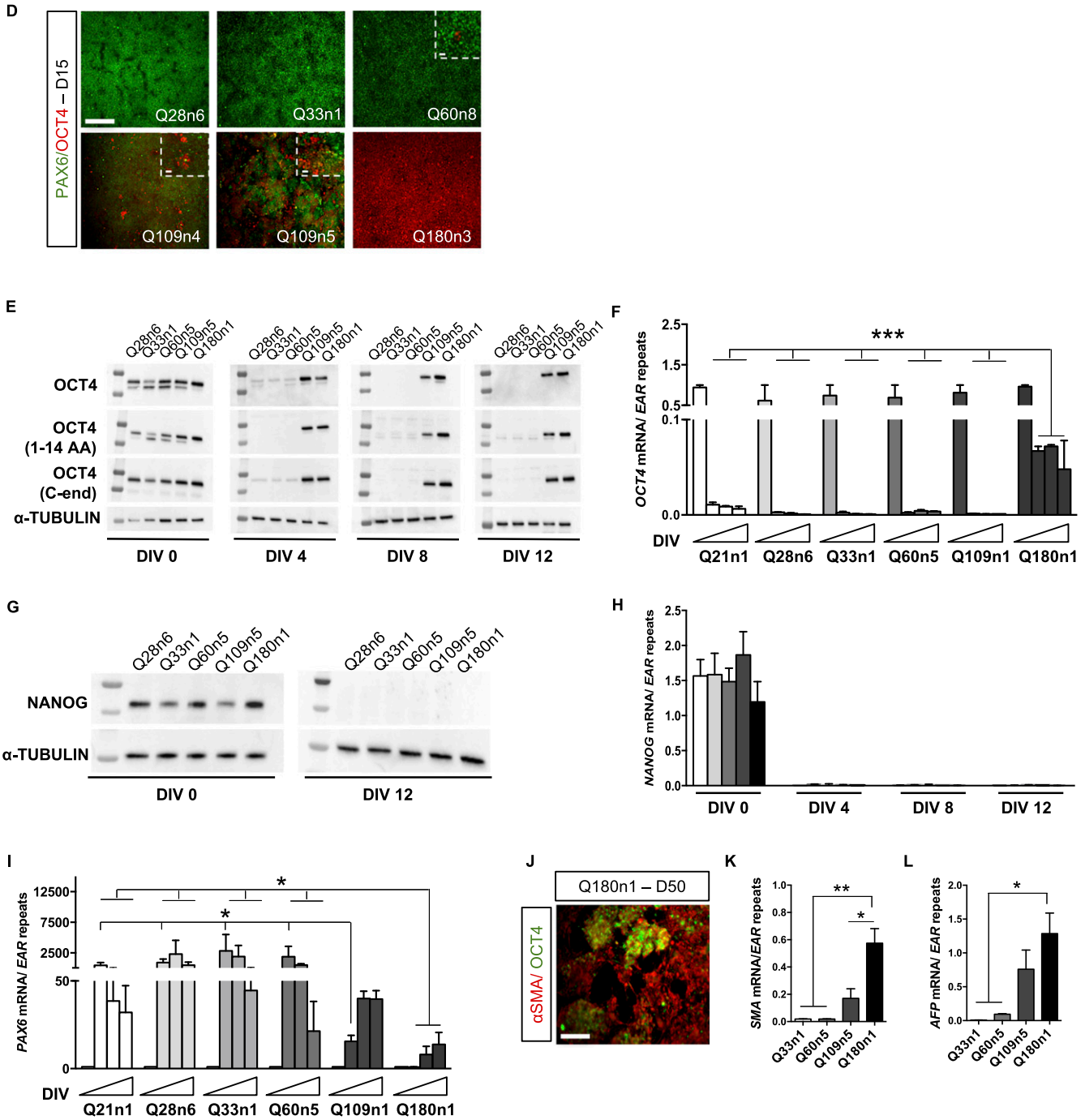

Fig. S1. (*A*) qPCR for total *HTT* mRNA in all lines/clones in self-renewal ($n = 3$ biological experiments, data are represented as mean ± SEM). (*B*) Scheme of striatal differentiation protocol applied to HD and CTR iPS cell lines. (*C*) Immunocytochemistry for OCT4 and SOX2 at DIV0 in CTR lines (Q21n1, Q28n6, and Q33n1) and in all HD lines/clones (Q60n5, Q60n8, Q109n1, Q109n4, Q109n5, Q180n1, and Q180n3). (Scale bar, 50 μm.) (*D*) Immunocytochemistry for OCT4 and PAX6 at DIV15 of differentiation in Q28n6, Q33n1, and additional clones of Q60n8, Q109n4, Q109n5, and Q180n3. (Scale bar, 100 μm.) The *Insets* show the presences of $OCT4^+$ cells also in these clones (crops of the same images). (Scale bar, 50 μm.) (*E*) Western blot analysis for OCT4 using three different antibodies able to recognize three different portions of the protein. Analysis was performed at DIV0, 4, 8, and 12 for two control lines (Q28n6 and Q33n1) and three HD lines (Q60n5, Q109n5, and Q180n1). α-Tubulin was run in the same samples. (*F*) qPCR for *OCT4* mRNA in all CTRs and HD cell lines during differentiation at DIV0, 8, 15, and 30. (A.U., $***P < 0.001$ one-way ANOVA; $n = 3$ biological experiments, data are represented as mean ± SEM.) (*G*) Western blot analysis for NANOG at DIV0 and 12 in CTRs Q28n6 and Q33n1 and HD lines in parallel with α-tubulin. (*H*) qPCR for *NANOG* mRNA in all CTRs and HD cell lines during differentiation at DIV0, 4, 8, and 12 ($n = 3$ biological experiments, data are represented as mean ± SEM). (*I*) qPCR for *PAX6* mRNA in all CTRs and HD cell lines during differentiation at DIV0, 8, 15, and 30. (A.U., mean CTR lines 1,410-fold increase vs. 15-fold in Q109n1 and 1.35-fold in Q109n1, $*P < 0.05$ one-way ANOVA; $n = 3$ biological experiments, data are represented as mean ± SEM.) (*J*) Immunocytochemistry for OCT4 and α-SMA of Q180n1 at DIV50 of differentiation. (Scale bar, 100 μm.) (*K*) qPCR for α-SMA and (*L*) AFP in Q33n1, Q60n5, Q109n5, and Q180n1 at DIV50 of differentiation. (A.U. $*P < 0.05$, $**P < 0.01$ one-way ANOVA; $n = 3$ biological experiments, data are represented as mean ± SEM.)

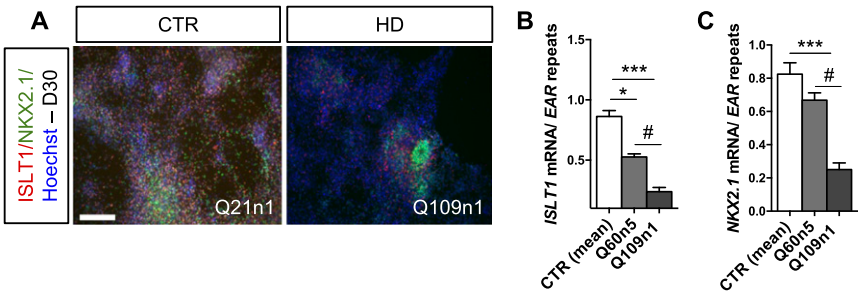

Fig. S2. (*A*) Double staining for the TFs ISLT1 and NKX2.1 in Q21n1 and Q109n1 at DIV30 of striatal differentiation protocol. (Scale bar, 100 μm.) (*B*) qPCR for *ISLT1* and (*C*) *NKX2.1* at DIV30 of CTRs and Q60n5 and Q109n1. (*NKX2.1*: CTRs = 0.83 ± 0.14; Q60n5 = 0.67 ± 0.06; Q109n1 = 0.27 ± 0.09; *ISLT1*: CTRs = 0.86 ± 0.1; Q60n5 = 0.52 ± 0.04; Q109n1 = 0.24 ± 0.05; $^{*}P < 0.05$, $^{***}P < 0.001$, $^{\#}P < 0.05$ one-way ANOVA; $n = 3$ biological experiments, data are represented as mean ± SEM.)

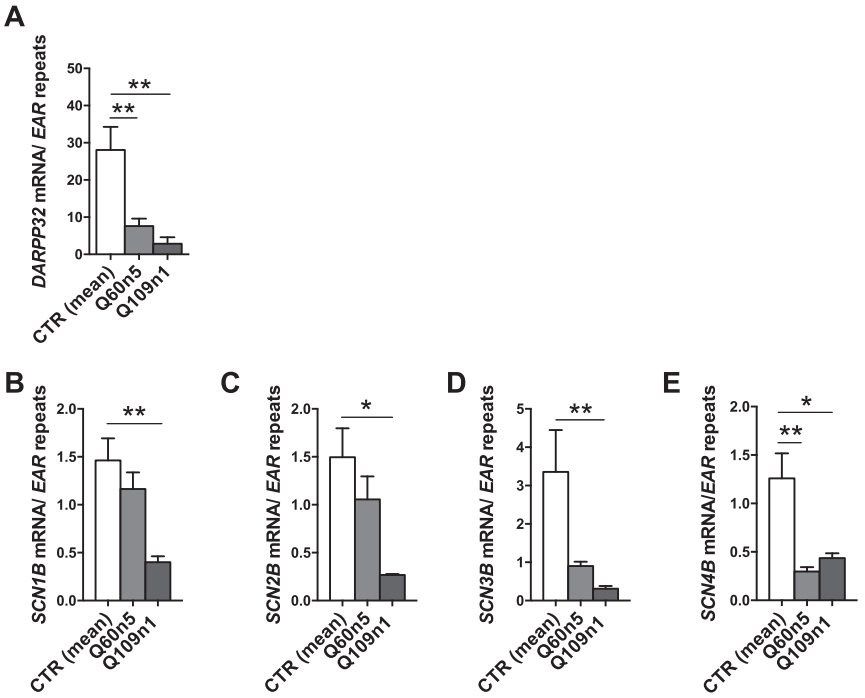

Fig. S3. (*A*) qPCR for *DARPP32* during differentiation at DIV0, 8, 15, and 30. MRNA level is normalized on *EAR* repeats. (A.U., CTRs = 28.3 ± 5.4; Q60n5 = 8.3 ± 1.13; Q109n1 = 3.5 ± 2.79; $^{**}P < 0.01$ one-way ANOVA; $n = 3$ biological experiments, data are represented as mean ± SEM.) (*B–E*) Gene expression analysis for Na^{+} channels (*B*) *SCN1B,* (*C*) *SCN2B,* (*D*) *SCN3B*, and (*E*) *SCN4B* evaluated at DIV30 of differentiation. Transcripts levels were normalized on *EAR* repeat level. (*SCN1B*, CTRs = 1.46 ± 0.65; Q60n5 = 1.16 ± 0.35; Q109n1 = 0.4 ± 0.13; *SCN2B*, CTRs = 1.42 ± 0.78; Q60n5 = 0.95 ± 0.48; Q109n1 = 0.3 ± 0.07; *SCN3B*: CTRs = 1.19 ± 0.37; Q60n5 = 0.73 ± 0.29; Q109n1 = 0.34 ± 0.18; *SCN4B*: CTRs = 1.06 ± 0.5; Q60n5 = 0.26 ± 0.07; Q109n1 = 0.43 ± 0.1; $^{*}P < 0.05$, $^{**}P < 0.01$ one-way ANOVA; $n = 3$ biological experiments, data are represented as mean ± SEM.)

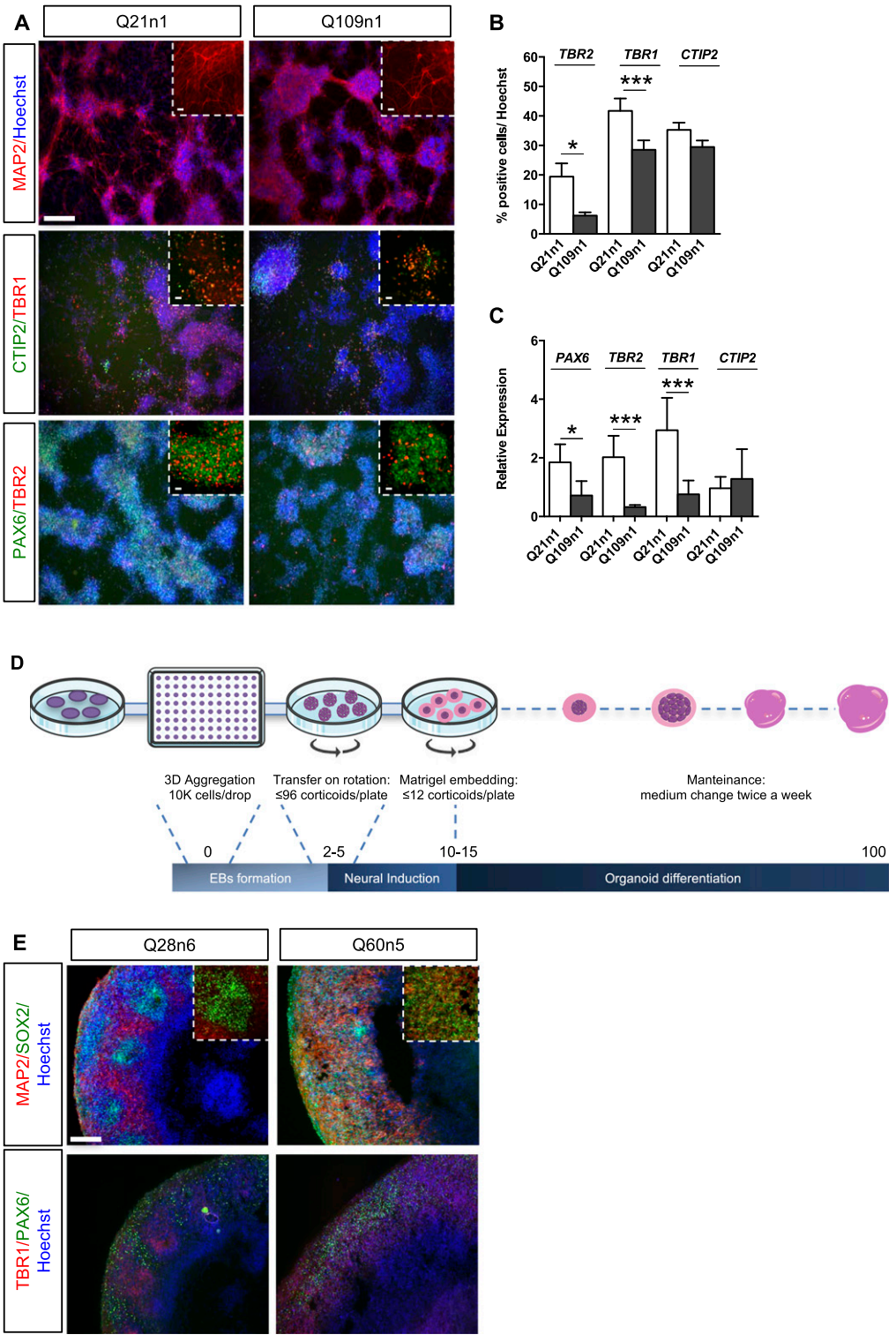

Fig. S4. (Continued)

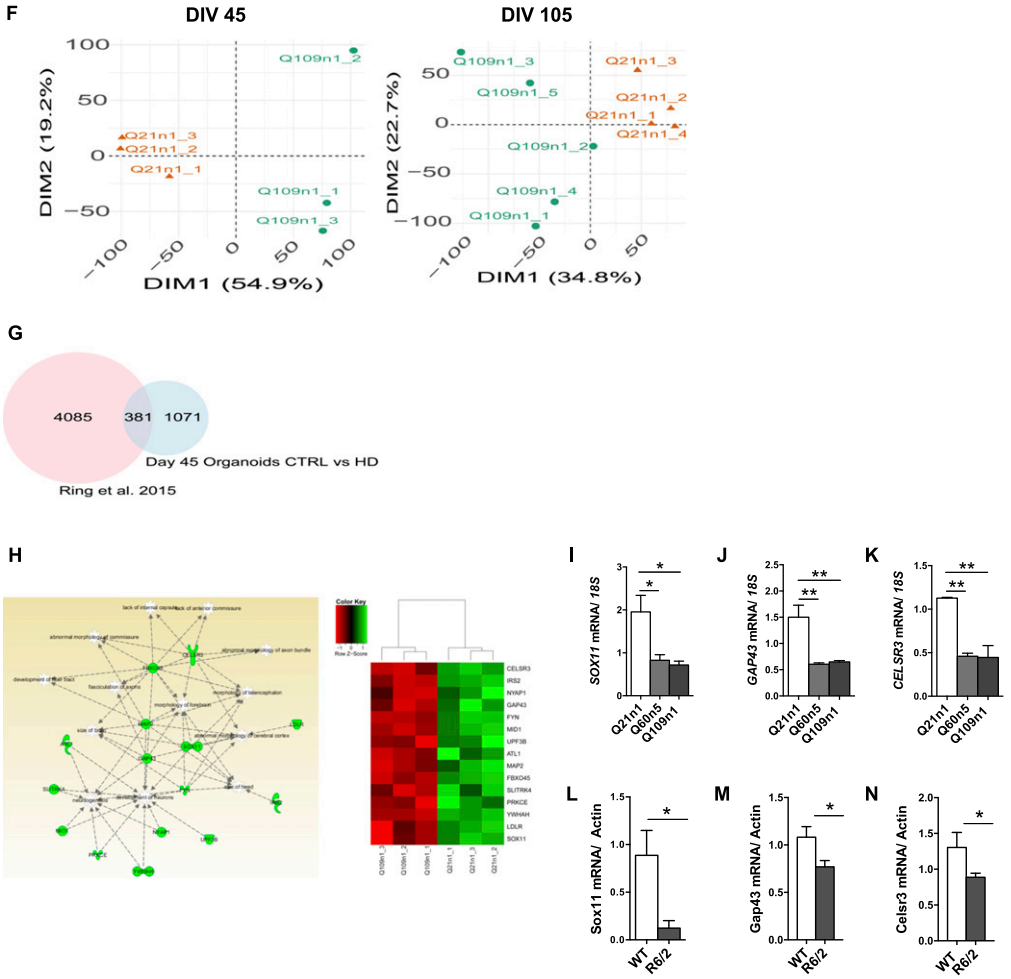

Fig. S4. (*A*) Representative images of DIV70 immunostaining for MAP2, CTIP2/TBR1 and PAX6/TBR2 on cultures of Q21n1 and Q109n1 after cortical differentiation. [Scale bar, 100 μm; *Inset* (crop of same images), 50 μm.] (*B*) Counts of TBR2$^+$, TBR1$^+$, and CTIP2$^+$ cells at DIV70 of differentiation performed using the ITCN ImageJ plugin. (*$P < 0.05$, ***$P < 0.001$ Student *t* test; $n = 3$ biological experiments, data are represented as mean ± SEM.) (*C*) Transcripts level normalized on *EAR* repeats for *PAX6, TBR2, TBR1*, and *CTIP2* at DIV70 of differentiation. (*PAX6*, CTR = 1.73 ± 0.69, Q109n1 = 1.11 ± 0.94; *TBR2*, CTR = 2.02 ± 0.73; Q109n1 = 0.32 ± 0.06; *TBR1*, CTR = 2.95 ± 1.1; Q109n1 = 0.76 ± 0.52; *CTIP2*, CTR = 0.96 ± 0.39; Q109n1 = 1.28 ± 1.01; *$P < 0.05$, ***$P < 0.001$ Student *t* test; $n = 3$ biological experiments, data are represented as mean ± SEM.) (*D*) Scheme of 3D differentiation protocol to obtain cerebral organoids from HD and CTR iPSC lines. (*E*) Organoids derived from Q28n6 and Q60n5 and double-stained for SOX2/MAP2 and for the cortical markers PAX6/TBR1. (Scale bar, 50 μm; magnification: *Insets*, 20×.) (*F*) PCA of DIV45 (*Left*) and DIV105 (*Right*) of both Q21n1 and Q109n1 cell lines. (*G*) Venn diagram showing the number of common DEGs between our CTR Q21n1 and HD Q109n1 organoids and the study performed by Ring et al. (22). (*H*, *Left*) Network with the highest-scored functional pathways; (*Right*) heatmap showing genes enriched for these pathways (*z*-score). (*I*) qPCR for *SOX11*, (*J*) *GAP43,* and (*K*) *CELSR3* mRNAs in 2D striatal cultures at DIV30 of differentiation. Transcript levels are normalized on the reference genes *18S*. (Each column represents the average of three independent differentiation protocols. A.U., *SOX11*: *$P < 0.05$; *GAP43*: *$P < 0.01$; *CELS3*: **$P < 0.01$ one-way ANOVA; $n = 3$ biological experiments, data are represented as mean ± SEM.) (*L*) qPCR for *Sox11*, *Gap43* (*M*), and *Cels3* (*N*) mRNAs on total brain from R6/2 and control mice at E16.5. Transcript levels are normalized on *Actin* mRNA level. In *L* and *M*, columns represent the average of three control mice and four R6/2 mice. (A.U., *Sox11*: *$P < 0.05$; *Gap43*: *$P < 0.05$; *Cels3*: *$P < 0.05$, Student *t* test; $n = 3$, data are represented as mean ± SEM.)

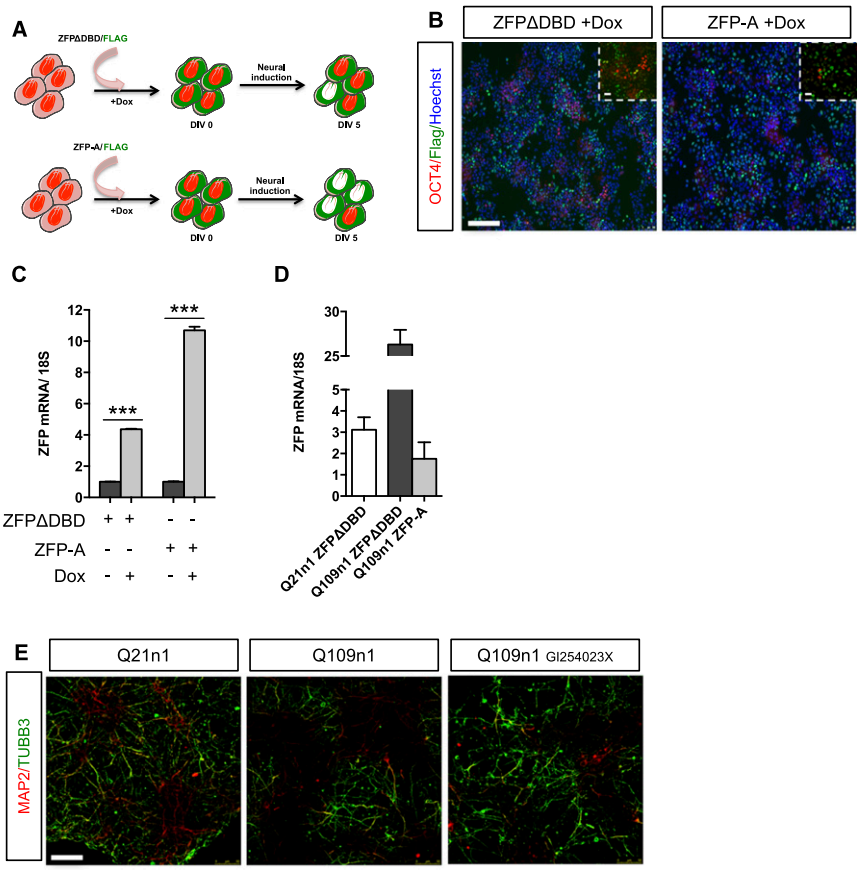

Fig. S5. (*A*) Schematic view of the experiment where cells expressing the inducible FLAG-tagged active ZFP-A or its inactive (ZFPΔDBD) version, are subjected to neural induction in presence of doxycycline (Dox). (*B*) Immunocytochemistry for OCT4 and FLAG in ZFP-expressing Q109n5 line at DIV5 of differentiation. (Scale bar, 100 μm; *Inset*, 50 μm.) (*C*) qPCR for ZFP mRNA expression in ZFPs-expressing Q109n5 lines after doxy treatment (+Dox) and relative control (−Dox) at DIV5 and 20 of differentiation. (A.U., $***P < 0.001$ Student *t* test; $n = 3$ biological experiments, data are represented as mean ± SEM.) (*D*) qPCR for ZFP mRNA in ZFP-A and ZFPΔDBD constitutive Q109n1 lines and ZFPΔDBD constitutive Q21n1 line at DIV8 and 30 of differentiation ($n = 3$ biological experiments, data are represented as mean ± SEM). (*E*) Immunostaining for TUBB3/MAP2 at DIV30 of differentiation after treatment with GI254023X. (Confocal images, scale bar, 50 μm.)

Table S1. Table of cell lines/clones utilized in this study

		Q-banding		Q-banding	
iPS line	Clone	Passage	Results	Passage	Results
Q21	**n 1**	p17	XX, 46	p36	XX, 46
Q28	n6	p20	XX, 46	p43	XX, 46
Q33	n1	p45	XX, 46	p67	XX, 46
Q60	n5	p25	XX, 46	p40	Abnormal
Q60	n8	p26	XX, 46	p43	Abnormal
Q109	n1	p35	XX, 46	p52	XX, 46
Q109	n4	p40	Abnormal	p49	Abnormal
Q109	n5	p34	XX, 46	p42	Abnormal
Q180	n1	p32	Abnormal	p65	Abnormal
Q180	n3	p53	Abnormal	p71	Abnormal

Cell lines were described in Mattis et al. (23). Cell lines were propagated for a maximum of 25–30 passages (3 mo) and then replenished. Karyotype was monitored every time after thawing by Q-banding. XX is referred to sexual chromosome, female; 46 is referred to the number of chromosomes.

Dataset S1. List of differentially expressed genes between CTR and HD organoids at DIV45 ($P < 0.01$)

Dataset S1

Dataset S2. List of differentially expressed genes between CTR and HD organoids at DIV45 that are common with the study performed in Ring et al. (22)

Dataset S2